

NEGATIVE ION PHOTOELECTRON SPECTROSCOPY OF TeO^- C.B. FREIDHOFF, J.V. COE, J.T. SNODGRASS,
K.M. McHUGH and K.H. BOWEN*Department of Chemistry, The Johns Hopkins University, Baltimore, MD 21218, USA*

Received 10 November 1985

We have recorded the photoelectron spectrum of TeO^- using a hot-cathode discharge ion source and a negative ion photoelectron spectrometer. The adiabatic electron affinity of TeO is determined to be 1.697 ± 0.022 eV. The negative ion parameters determined in this work are: $\omega_e''(\text{TeO}^-) = 690 \pm 80$ cm^{-1} , $r_e''(\text{TeO}^-) = 1.884 \pm 0.028$ Å, and $D_0(\text{TeO}^-) = 3.63 \pm 0.15$ eV.

1. Introduction

Substantial spectroscopic data are available about the TeO molecule [1–9]. TeO appears to have first been observed in 1938 by Shin-Piaw in emission spectra [2]. Subsequent spectroscopic work has included emission studies in the visible and in the near-ultraviolet [3–5], absorption in the near-ultraviolet [6], matrix-isolation studies in the infrared [7], and chemiluminescence in the near-infrared [8]. TeO is distinguished from other group VIB diatomic oxides by its unusually large spin–spin splitting in the ground state [8,10]. Thermochemical data on TeO are also available [11–13]. In contrast to TeO, very little information is available about its negative ion, TeO^- . We are aware of only one observation of TeO^- . This was by Constantinescu et al. who observed its ESR signal [14].

Here, we report the recording of the photodetachment spectrum of TeO^- by negative ion photoelectron spectroscopy. We obtain a highly structured spectrum for TeO^- from which the adiabatic electron affinity of TeO and the spectroscopic parameters B_e'' and ω_e'' for TeO^- are determined. Using these data, we also calculate r_e'' and D_0 for TeO^- .

2. Experimental

In negative ion photoelectron spectroscopy, a mass-selected negative ion beam is crossed with a fixed-fre-

quency laser beam under field-free and collision-free conditions and the resulting photodetached electrons are subjected to energy analysis. The difference between the photon energy and the center-of-mass electron kinetic energy of a given feature in the photoelectron spectrum corresponds to the transition energy from an occupied negative ion energy level to a level in its neutral counterpart. Our apparatus, which has been discussed previously [15], employs a Wien ($E \times B$) velocity filter for mass selection, an argon ion laser operated intracavity through the ion–photon interaction region, and a magnetically shielded hemispherical electron energy analyzer.

The ion source used in this work was a hot-cathode discharge (Branscomb) source modified for use at higher temperatures than usual. In this source a ThO_2/Ir filament was used to produce an electrical discharge from which various negative ions were extracted [16]. A second filament (W) was used to heat solid samples in an alumina boat positioned near the discharge region. To generate TeO^- , tellurium powder was placed in the boat below the heater filament. Nitrous oxide was used as the emission support gas and as the source of oxygen to form TeO^- and TeO_2^- . With the heater filament off, the typical ions formed from N_2O in a Branscomb source were seen, i.e. O^- , OH^- , NO^- , O_2^- , and NO_2^- . With the heater filament turned on the main ions formed were O^- , OH^- , NO^- , Te^- , TeO^- , and TeO_2^- . A typical mass spectrum is shown in fig. 1.

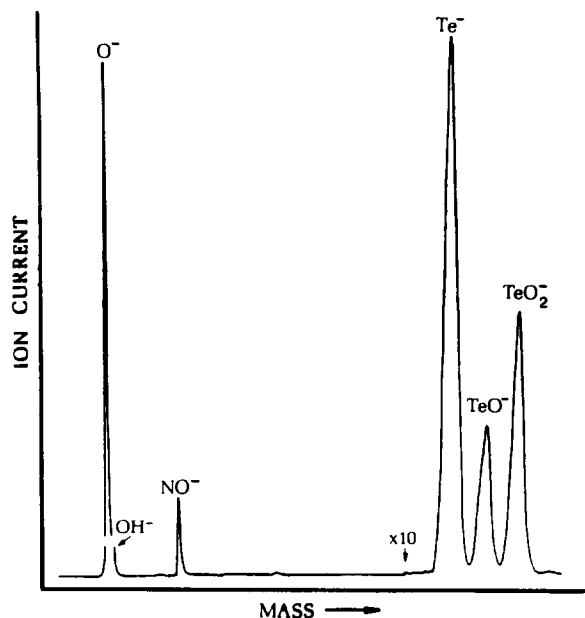


Fig. 1. A negative ion mass spectrum showing the ions generated by a hot-cathode discharge (Branscomb) source during these experiments.

3. Results and discussion

3.1. Data for TeO^-

Our photoelectron spectrum of TeO^- , which was recorded with 2.540 eV photons, is presented in fig. 2. A photoelectron spectrum of O_2^- was taken at the beginning and end of each day to check the transmission function of the electron energy analyzer. The singlet-triplet splitting in O_2^- was used to provide an energy scale compression factor. The ions O^- and Te^- were photodetached both before and after each spectral run in order to calibrate the TeO^- spectra. The instrumental resolution employed in these experiments was ≈ 30 meV. To obtain peak centers and heights of optimal accuracy, the raw data peaks were fit to an asymmetric Gaussian function prior to analysis.

3.2. Spectral assignment

Among the lighter group VIB diatomic oxides the low-lying electronic states of the neutrals are designated as $X^3\Sigma^-$, $a^1\Delta$, and $b^1\Sigma^+$ since they are coupled ac-

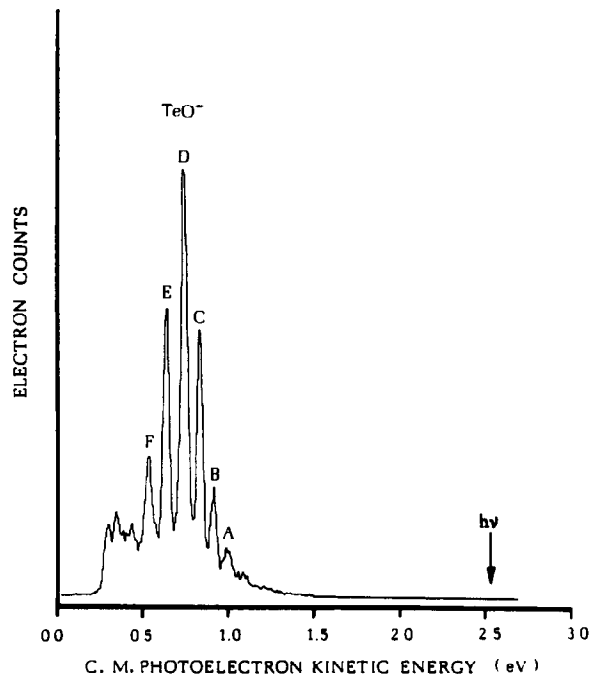


Fig. 2. The photoelectron spectrum of TeO^- presented in terms of center-of-mass electron kinetic energies. This spectrum was recorded over approximately one hour with 0.030×10^{-9} A of TeO^- ion current and 230 W of 2.540 eV photons. The channel spacing of the spectrum is 8.4 meV.

ording to Hund's case "a" or "b". In contrast to these, however, TeO is believed to be coupled according to Hund's case "c" [8]. In case "c" the $X^3\Sigma^-$ state becomes XO^+ and $X1^\pm$, a $^1\Delta$ becomes a 2, and $b^1\Sigma^+$ is $b0^+$. As mentioned earlier TeO possesses a relatively large ground state spin-spin splitting which has been determined to be 789 cm^{-1} [8]. By comparison, little is known about the magnitude of the spin-orbit splitting in the negative ion TeO^- . Some guidance in estimating its magnitude is provided by the isoelectronic neutral molecule IO in which the spin-orbit splitting is thought to be ≈ 0.3 eV [1]. On this basis we assume that the spin-orbit splitting in TeO^- is also rather large. In referring to the upper and lower spin-orbit states of TeO^- , we have used the case "c" state designations $X1/2$ and $X3/2$ strictly as a nomenclature of convenience.

The photoelectron spectrum of TeO^- is complicated by the fact that the spin-spin splitting in the ground state of TeO is essentially equal to the $\Delta G_{1/2}$

values ($\approx 790 \text{ cm}^{-1}$) of both the $X 0^+$ and the $X 1^\pm$ states in TeO. The consequence of this is that the $X 1^\pm(v')$ vibrational levels occur within a few wavenumbers of the $X 0^+(v' + 1)$ vibrational levels and that, at an instrumental resolution of $\approx 30 \text{ meV}$ (240 cm^{-1}), transitions to these levels are unresolved. Also, since the $X 1^\pm$ state is doubly degenerate transitions to it are twice as strong as are those to the lower energy [8] $X 0^+$ state. If the spin-orbit splitting in the TeO^- negative ion is as large as we have assumed, then its upper spin-orbit state is not expected to be significantly populated, and those transitions that do appear due to the upper state will be shifted to the high electron kinetic energy side of the main spectral profile. Transitions from the first few vibrationally excited levels of the lower TeO^- spin-orbit state to the various vibrational/spin-spin states of TeO are, however, expected to be very much in evidence. The effects of such hot bands should be greatly amplified in this particular system due not only to the coincidence of the vibrational spacings with the spin-spin splitting in TeO, but also to the two-fold degeneracy of the $X 1^\pm$ state of TeO. Thus, even a modest occurrence of hot bands can be expected to distort the spectral profile considerably.

Table 1 presents center-of-mass electron kinetic energies of the peak centers for peak A through F as well as adjacent peak spacings and our assignments. The spacing between peak couples C/D, D/E, and E/F are all roughly equal to the expected spacings in the

neutral, i.e. $\approx 790 \text{ cm}^{-1}$. While the successive increases in spacing from peak C to F could suggest a negative anharmonicity, they are actually the result of hot band pulling effects as will be seen below. The spacings between peak couples A/B and B/C are somewhat smaller. These observations are consistent with the assignments of peaks A-F that are shown in table 1. Under this interpretation peak C contains the $\text{TeO}(X 0^+(v' = 0)) \leftarrow \text{TeO}^-(X 3/2(v'' = 0))$ transition, i.e. the origin. Peak A and B (and a portion of C) are hot bands whose relative intensities vary with source conditions. One expects the spacings between these hot band peaks to be smaller than the others because an electron that is added to TeO goes into an antibonding orbital. This results in a TeO^- bond length $r_e''(\text{TeO}^-)$ that is longer than in the TeO neutral and a vibrational frequency for the ion $\omega_e''(\text{TeO}^-)$ that is smaller than in the neutral.

In order to confirm this assignment and to obtain spectroscopic parameters for TeO^- , we next modeled the TeO^- photoelectron spectrum. Since peak B was felt to be the next most likely contender for the origin peak after peak C, comparative modeling was conducted assuming both assignments. When spectral modeling was done on the assumption that peak B was the origin peak, the agreement with the observed spectrum was poor. But when the modeling was conducted on the assumption that peak C was the origin peak, there was good agreement with the observed spectrum. In an effort to investigate the capability of hot bands to

Table 1
Peak locations, spacings, and assignments of the TeO^- photoelectron spectrum

Peak	c.m. electron kinetic energy (eV)	Adjacent peak spacings (cm^{-1})	Assignment (v', v'') $\text{TeO}(X 0^+ \text{ or } X 1^\pm(v')) \leftarrow \text{TeO}^-(X 3/2(v''))$	
			$X 0^+$	$X 1^\pm$
A	0.982	605	(0,2)	(0,3)
B	0.907		(0,1)	(0,2)
C	0.829	750	(0,0)	(0,1)
D	0.736		(1,0)	(0,0)
E	0.633	831	(2,0)	(1,0)
F	0.528		(3,0)	(2,0)

distort peak heights and to pull peak centers, we also modeled the spectrum on the assumptions that peak C was the origin peak and that there were no hot band contributions. Under these circumstances we found that the peak-height ratio of peak C to peak D was reduced to almost 1 : 3. As anticipated, the height of the origin peak in this system is seen to be substantially influenced by hot bands. We also found strong hot band pulling effects on peaks E and F that explained the anomalously large D/E and E/F peak spacings. These modelings have thus reaffirmed our conclusions that peak C contains the origin transition and that the assignments in table 1 are the proper ones.

The negative ion potential parameters for TeO^- which were obtained from the best fit are: $\omega_e'' = 690 \pm 80 \text{ cm}^{-1}$, $B_e'' = 0.334 \pm 0.010 \text{ cm}^{-1}$, and therefore $r_e'' = 1.884 \pm 0.028 \text{ \AA}$. The TeO^- vibrational populations were found to be decidedly non-Boltzmann with the higher v'' levels exhibiting higher "temperatures". These "temperatures" were calculated by comparing the intensities of individual hot bands with those of adjacent (lower v'') peaks. The average of such "temperatures" over the first several hot bands was $\approx 1300 \pm 500 \text{ K}$.

Barrow and Lemanczyk [17] have observed that diatomics with the ground state configuration $\dots\pi^2$ have a ratio of the term energies for their $a^1\Delta$ and $b^1\Sigma^+$ states of 0.55 ± 0.05 . Winter et al. [8] have measured the $b^0 \rightarrow X_1^0$ transition energy in TeO to be 9966 cm^{-1} . This predicts that the origin peak of the a^2 state will lie at a c.m. electron kinetic energy of $\approx 0.15 \text{ eV}$ in our photoelectron spectrum. Of necessity, electron-energy analyzers have low-electron-energy "cut-offs", and ours typically occurs between 0.2 and 0.3 eV. For this reason we should not and we do not observe transitions from the main part of the a^2 manifold. The features to the low-electron-energy side of peak F, however, may be due to hot band transitions from the negative ion to the a^2 state of TeO.

3.3. Electron affinity of TeO

The adiabatic electron affinity of TeO was calculated from

$$\begin{aligned} \text{EA}(\text{TeO}) = & \text{EA}(\text{A}) + \gamma [\Omega(\text{A}^-) - \Omega(\text{TeO}^-)] \\ & + mW [1/M(\text{A}) - 1/M(\text{TeO})], \end{aligned} \quad (1)$$

where $\text{EA}(\text{A})$ is the electron affinity of Te or O, γ is the energy scale compression factor, $\Omega(\text{A}^-)$ is the laboratory electron kinetic energy position for the $\text{O}(^3\text{P}_2) \leftarrow \text{O}^-(^2\text{P}_{3/2})$ or the $\text{Te}(^3\text{P}_2) \leftarrow \text{Te}^-(^2\text{P}_{3/2})$ transitions [18,19], $\Omega(\text{TeO}^-)$ is the laboratory electron energy for the $\text{TeO}(\text{X } 0^+(v' = 0)) \leftarrow \text{TeO}^-(\text{X } 3/2(v'' = 0))$ transition in the TeO^- spectrum (peak C), m is the mass of an electron, W is the beam energy, and $M(\text{A})$ and $M(\text{TeO})$ are the respective masses of $\text{A} = \text{Te}$ or O and TeO . Making these determinations in this manner relative to a calibrant ion with a known electron affinity compensates for any contact potential corrections, and the last term in this equation provides a kinematic correction from laboratory electron energies to center-of-mass electron kinetic energies. The value of $\text{EA}(\text{TeO})$ determined from this equation was $1.709 \pm 0.008 \text{ eV}$, where the uncertainty is the experimental uncertainty. Corrections to this value may arise due to the effects of hot band pulling, rotational state populations, and the spin-orbit splitting in TeO^- . Transitions from excited vibrational states of TeO^- , which add asymmetrically to the height of peak C shift its location to lower electron kinetic energies by 7.8 meV, thus adding a correction of -7.8 meV to the electron affinity. To make a rotational correction, we assumed a Boltzmann distribution and a rotational temperature equal to the vibrational "temperature" of 1300 K mentioned earlier. At this rotational "temperature" the most prevalent rotational state in the negative ions is $J''(\text{max}) \approx 36$. An approximate rotational energy correction is then given [20] by

$$(B_e'' - B_e') J''(\text{max}) [J''(\text{max}) + 1], \quad (2)$$

where B_e'' and B_e' are the rotational constants of the ground electronic states of TeO^- and TeO , respective-

Table 2
Electron affinities of the group VIB atoms and their diatomic monoxides

Group VIB atoms ^{a)} (eV)	Group VIB oxides ^{b)} (eV)
O(1.462)	O ₂ (0.440)
S(2.077)	SO(1.126)
Se(2.021)	SeO(1.456)
Te(1.971)	TeO(1.697)

a) Ref. [22]. b) Refs. [15,20,21].

Table 3
Summary of selected spectroscopic parameters for the group VIB diatomic monoxides and their negative ions

Oxide system	Rotational constants (cm^{-1})		Vibrational frequencies (cm^{-1})	
	neutral ^{a)} B'_e	ion ^{b)} B''_e	neutral ^{a)} ω'_e	ion ^{c)} ω''_e
O ₂	1.4456	1.17	1580	1090
SO	0.7208	0.643	1149	895
SeO	0.4710	0.425	915	730
TeO	0.3561	0.334	798	690

a) Ref. [1]. b) Refs. [15,20,21]. c) Refs. [1,15,21].

ly. This correction is -3.7 meV. The assumed spin-orbit splitting in TeO^- is so large that the upper spin-orbit state is not expected to cause an appreciable shift in the location of peak C. For this reason no spin-orbit correction is applied. The combination of all these corrections and uncertainties gives a value for the adiabatic electron affinity of TeO as 1.697 ± 0.022 eV.

3.4. Bond dissociation energy of TeO^-

Given the electron affinities of Te and TeO and the dissociation energy of TeO, the dissociation energy of TeO^- can be calculated from a thermochemical cycle. Using $\text{EA}(\text{Te}) = 1.9708$ eV [19] and $D_0(\text{TeO}) = 3.90 \pm 0.15$ eV [1,7,11] we obtain 3.63 ± 0.15 eV for the dissociation energy of TeO^- into the ground states of Te^- and O.

3.5. Periodic trends among the group VIB diatomic monoxides

TeO^- is the fourth group VIB diatomic monoxide negative ion to have been studied by negative ion photoelectron spectroscopy [15,20,21]. Table 2 compares the electron affinities of the group VIB atoms with those of their diatomic monoxides. The electron affinities of the oxides are smaller than those of their atoms. As one proceeds down the group VIB column, the electron affinities of the monoxides both increase in magnitude and approach more closely the electron affinities of their heavy atoms. This latter trend is also seen in the group VIB diatomic hydrides [23]. Table 3 compares the rotational constants and the vibrational frequencies for the group VIB diatomic monoxides

and their negative ions. Both the rotational constants and the vibrational frequencies of the ions are smaller than those of their neutrals. As one proceeds down the group VIB column, both the rotational constants and the vibrational frequencies of the ions decrease in magnitude and approach more closely the rotational constants and vibrational frequencies of their corresponding neutrals. The properties of TeO^- are thus seen to conform reasonably well to the trends set by its analogs.

Acknowledgement

We have benefited from discussions on TeO^- with Paul Dagdigian and Betty Gaffney. This research was supported in part by the Research Corporation, and by BRSO Grant S07 RR07041 awarded by the Biomedical Research Support Grant Program, Division of Research Resources, National Institutes of Health. Acknowledgement is also made to the Donors of The Petroleum Research Fund, administered by the American Chemical Society, for partial support of this research.

References

- [1] K.P. Huber and G. Herzberg, *Molecular spectra and molecular structure. IV. Constants of diatomic molecules* (Van Nostrand Reinhold, New York, 1979).
- [2] Choong Shin-Piaw, *Ann. Phys. (Paris)* 10 (1938) 173.
- [3] R.L. Pulbrick, *J. Chem. Phys.* 30 (1959) 962.
- [4] P.B.V. Haranath, P.T. Rao and V. Sivaramamurty, *Z. Physik* 155 (1959) 507.
- [5] G.G. Chandler, H.J. Hurst and R.F. Barrow, *Proc. Phys. Soc.* 86 (1965) 105.

- [6] R.F. Barrow and H.J. Hurst, *Nature* 201 (1964) 699.
- [7] D.W. Muenow, J.W. Hastie, R. Hauge, R. Bautista and R.L. Margrave, *Trans. Faraday Soc.* 65 (1969) 3210.
- [8] R. Winter, I. Barnes, E.H. Fink, J. Wildt and F. Zabel, *J. Mol. Struct.* 80 (1982) 75.
- [9] A.W. Potts and T.A. Williams, *Chem. Phys. Letters* 42 (1976) 550.
- [10] R.F. Barrow and M.R. Hitchings, *J. Phys.* B5 (1972) L132.
- [11] H.G. Staley, *J. Chem. Phys.* 52 (1974) 4311.
- [12] V. Piacente, L. Malaspina and G. DeMaria, *Corsi. Semin. Chem.* 13 (1968) 53.
- [13] K.F. Zmbov and M.M. Miletic, *Glas, Hem. Drus. Beograd.* 43 (1978) 521.
- [14] O. Constantinescu, I. Pasaru and M. Constantinescu, *Rev. Roum. Phys.* 12 (1967) 223.
- [15] J.V. Coe, J.T. Snodgrass, C.B. Freidhoff, K.M. McHugh and K.H. Bowen, *J. Chem. Phys.*, to be published.
- [16] L.M. Branscomb, D.S. Burch, S.J. Smith and S. Geltman, *Phys. Rev.* 111 (1958) 504.
- [17] R.F. Barrow and R.Z. Lemanczyk, *Can. J. Phys.* 53 (1975) 553.
- [18] H. Hotop and W.C. Lineberger, *J. Phys. Chem. Ref. Data* 4 (1975) 539.
- [19] J. Slater and W.C. Lineberger, *Phys. Rev. A* 15 (1977) 2277.
- [20] R.J. Celota, R.A. Bennett, J.L. Hall, M.W. Siegel and J. Levine, *Phys. Rev. A* 6 (1972) 631.
- [21] W.C. Lineberger, in: *Laser spectroscopy*, eds. R. Brewer and A. Mooradian (Plenum Press, New York, 1974).
- [22] R.D. Mead, A.E. Stevens and W.C. Lineberger, in: *Gas phase ion chemistry*, Vol. 3, ed. M.T. Bowers (Academic Press, New York, 1984).
- [23] C.B. Freidhoff, J.T. Snodgrass, J.V. Coe, K.M. McHugh and K.H. Bowen, *J. Chem. Phys.*, to be published.